Absolute Instability Competition and Suppression in a Millimeter-Wave Gyrotron Traveling-Wave Tube

Larry R. Barnett, Lung Hai Chang, Han Ying Chen, Kwo Ray Chu,
Wai Keung Lau, and Chuan Cheng Tu

Department of Physics, National Tsing Hua University, Hsinchu, Taiwan, Republic of China

(Received 3 April 1989)

Harmonic absolute instability in the TE_{21} mode is found to cause mode competition in a new millimeter-wave gyrotron traveling-wave tube experiment designed for high stability in the TE_{11} mode. Complete suppression of this instability by the application of the TE_{11} drive has been observed with beam currents up to at least 6 times the instability threshold, which results in high amplified power (~25 kW) at high efficiency (~23%). The study is significant in that it demonstrates that cyclotron-maser amplifiers may operate at a current well above oscillation threshold without degradation in saturated performance.

PACS numbers: 42.52.+x, 85.10.Jz

The gyrotron traveling-wave tube (gyro-TWT) has far greater power-handling capability than the TWT, yet its susceptibility to oscillations has been a well-known factor limiting the power achieved in experiments.[1-5] The Naval Research Laboratory[2] reported a 35-GHz, TE_{01}-mode gyro-TWT with 16.6-kW output power at 7.8% efficiency. A 95-GHz TE_{11}-mode gyro-TWT was tested at Varian Associates, producing output power of over 20 kW with 30-dB gain, 8% efficiency, and 2% electronic bandwidth.[6] In the *C* band, 120 kW at 26% efficiency was reported by Varian.[4,5] Theoretical and experimental investigations[4,7] revealed that the absolute instability (in the operating mode or a different mode) and end reflections (near the cutoff frequency of the operating mode) were the two dominant causes of oscillations in a gyro-TWT. While the reflection oscillation can be remedied by improved input-output match, avoidance of the intrinsic absolute instability requires more basic considerations. Investigations[7,8] showed that the amplifier stability greatly improved with increasing beam voltage V_b and decreasing α ($=v_\perp/v_\parallel$). It is for this reason that the current experiment was designed for a relatively high voltage ($\simeq$95 kV) and low α ($\simeq$1). A *single-anode* magnetron injection gun (MIG)[9,10] with simulated beam axial velocity spread $<4\%$ was used (for the first time in a gyro-TWT). The design magnetic field ($B_0=12.5$ kG) was 2% below grazing (Fig. 1) for higher efficiency,[11,12] and the design current ($I_b=2$ A) was 40% of the calculated threshold of the TE_{11}-mode absolute instability.

The experimental configuration is shown in Fig. 2. The input coupler is a matched $TE_{10}^{\square}$-to-TE_{11}° (linear polarization) converter followed by a 2.5-cm slightly elliptical section tilted at 45° to generate circular polarization. It has two $TE_{10}^{\square}$ input ports 90° apart to generate either right- or left-circular polarization depending on which port is excited. The coupler works exceptionally well in that the loss from $TE_{10}^{\square}$ to TE_{11}° (circular polarization) is ~0.2 dB (virtually all due to Ohmic loss) and the isolation between left- and right-circular polarization is of the order of 30 dB or better. An identical coupler is used on the output to separate the rf from the beam. The total transmission loss, window to window, is ~0.8 dB. The couplers provide an additional benefit of critical importance in studies of oscillations. By separating the TE_{11} circularly polarized wave from non-TE_{11} circularly polarized waves, the couplers allow even very-low-level oscillations to be observed, at both the input and output, without interference from a large-amplitude TE_{11} circularly polarized wave. The interaction waveguide with a radius (r_w) of 0.2654 cm and a length of 17.5 cm is connected to the couplers (radius=0.318 cm) by 1.2-cm tapers. Beam transmission from gun to collector is 100%.

The frequency of operation is 34.712 GHz set by our fixed-frequency magnetron driver. All input and output powers presented below are measured, respectively, at the input and output windows by carefully calibrated (mismatch and transfer errors are minimized) directional-coupler, crystal-detector systems with estimated accuracies of approximately ±5%.

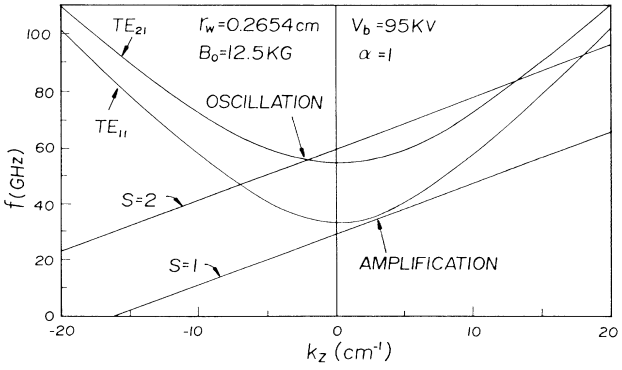

FIG. 1. Dispersion curves for the TE_{11} and TE_{21} modes, and the beam resonance lines at the fundamental ($s=1$) and second ($s=2$) cyclotron harmonics.

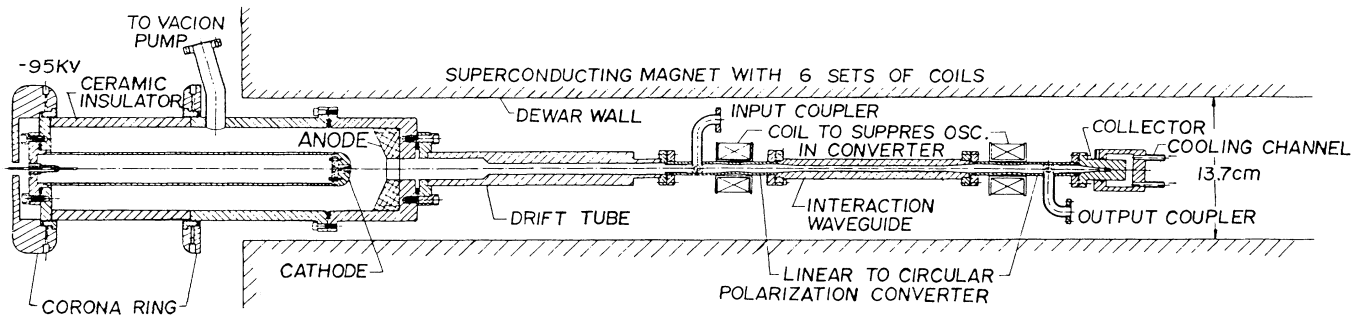

FIG. 2. Schematic of the gyro-TWT. There are two input ports and two output ports (only one is shown).

Figure 3(a) shows the amplified power (all at output port 1) versus input power at $I_b = 0.26$ A. The curve follows close to a classical linear small-signal region with a saturation peak of ~ 4.6 kW at ~ 170-W drive except for a small nonlinear bump in gain at (20–30)-W drive. An oscillation at ~ 56.8 GHz (measured by an interferometer with an estimated accuracy of $\pm 0.2\%$) is observed at output port 2. From Fig. 1, we may identify the oscillation as a TE_{21} absolute instability at the second cyclotron harmonic. The oscillation power is much weaker, the *relative* amplitude of which is also plotted. Note that the bump increase in gain coincides with a rapid drop in oscillation power. At 30-W

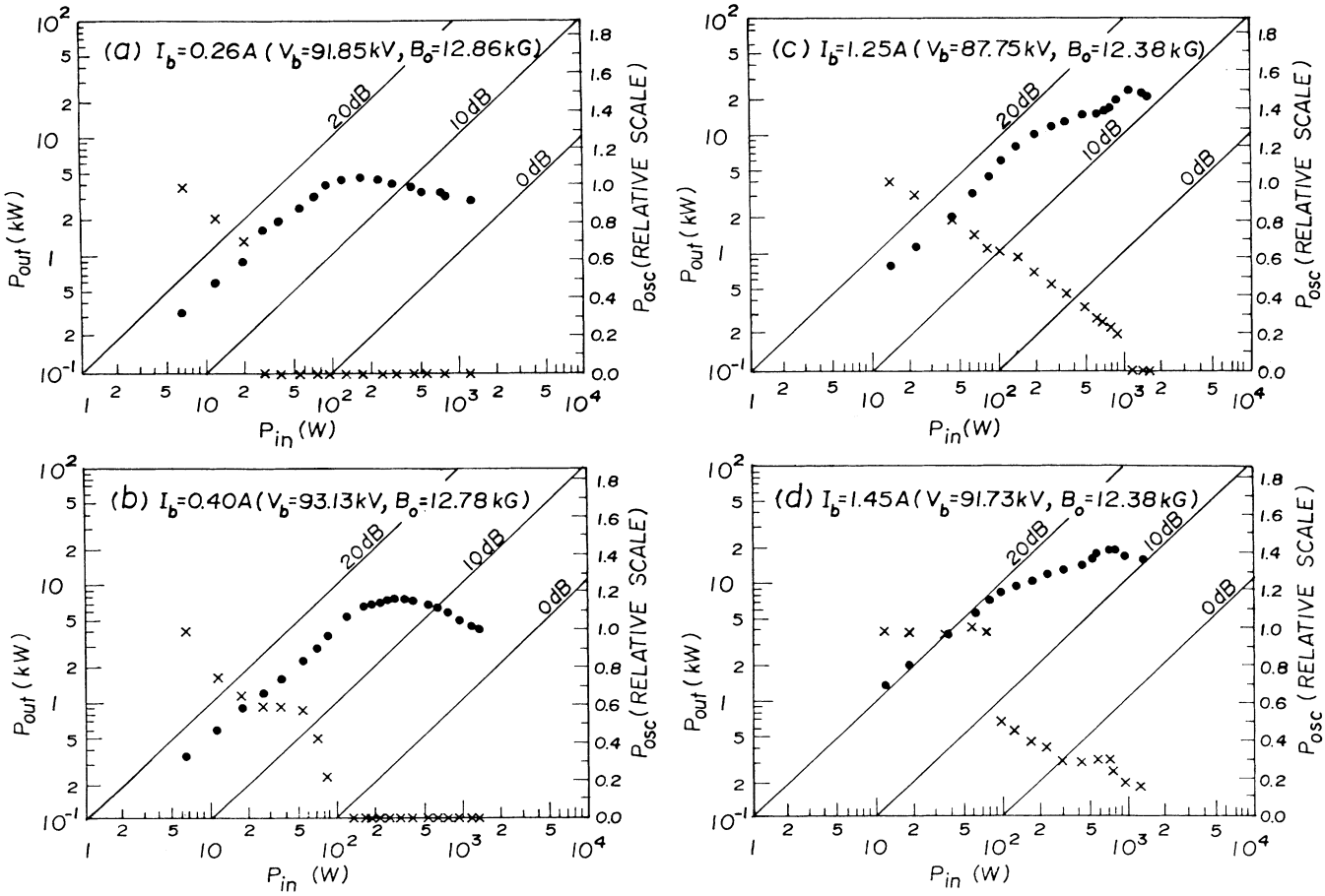

FIG. 3. The amplified TE_{11} output power (filled circles, on absolute scale) and the TE_{21} oscillation power (crosses, on relative scale) vs the TE_{11} drive for (a) $I_b = 0.26$ A, (b) $I_b = 0.40$ A, (c) $I_b = 1.25$ A, and (d) $I_b = 1.45$ A. Other parameters (in parentheses in each figure) are adjusted slightly for maximum efficiency. In some cases other than (a)–(c), the suppressed oscillation reappears at still higher drive.

drive, the TE_{21} oscillation is completely gone. This behavior provides unambiguous evidence of mode competition and suppression in a gyro-TWT.

Figure 3(b) shows a similar behavior for $I_b = 0.4$ A, but now 130 W of drive is required for complete suppression of the TE_{21} oscillation. The peak amplified power occurs after the oscillation is suppressed and, as in Fig. 3(a), the efficiency is not degraded.

Our best power and efficiency, 24.9 kW at $\eta \simeq 23\%$ for $I_b = 1.25$ A, are shown in Fig. 3(c). The TE_{21} oscillation now occurs at two frequencies (55.2 and 56.0 GHz) and is more powerful. Complete suppression of the oscillation requires ~ 1 kW of drive which is also the input power for maximum efficiency. Thus, 1.25 A appears to be the maximum beam current for which the peak efficiency is not degraded by oscillation. As the beam current is raised further [e.g., Fig. 3(d)], the powerful oscillations can only be partially suppressed with the drive power available. Also, the peak power is degraded by the competing oscillations.

The TE_{21} oscillation has a threshold current (I_{th}) of ~ 0.2 A. Its power level at 1.25 A (with zero rf drive), as measured by a calorimeter, is 1.7 kW $\pm$ 3 dB. The 3-dB uncertainty is mainly due to the uncertainty of 55-GHz losses in the overmoded WR28 waveguides. In the beam current range of Fig. 3, the TE_{21} power is found to be approximately proportional to $I_b - I_{th}$, as observed by a crystal detector.

Figure 4 is a compilation of power and efficiency versus I_b. The increase of P_{out} and η with I_b (up to 1.25 A) is in reasonable agreement with the crude theoretical scaling relation $\eta \sim I_b^{1/3}$ for low beam current. At 1.3 A and beyond, the TE_{21} oscillations become too strong to be completely suppressed by the drive and η drops suddenly from $\sim 23\%$ to $\sim 13\%$. Thus, competition with oscillations appears to explain the departure from the theoretical scaling in many early observations. It is interesting to note that Fig. 4 predicts much greater power if further suppression of the TE_{21} oscillation can be achieved (e.g., by a sever).

As discussed before, output port 1 couples out both the amplified TE_{11} wave and the TE_{21} oscillation, while port 2 couples out only the TE_{21} oscillation. Figure 5 shows oscilloscope photos of the output signals for the conditions of Fig. 3(c). Figure 5(a) is the output detector signal from port 1 with the amplified TE_{11} wave ($\sim \frac{1}{2}$-μsec pulse) flanked by the TE_{21} oscillations on both sides [cf. Fig. 5(e)]. Figure 5(b) uses notch filters to reject the TE_{21} oscillations in Fig. 5(a), showing 24 kW of TE_{11} output with 870-W drive. Figure 5(c) is the TE_{21} oscillation observed at port 2 with no drive applied. Figure 5(d) is from port 2 with 220-W drive applied which results in ~ 6-dB suppression during the $\frac{1}{2}$-μsec driver pulse. Figure 5(e) is from port 2 with the 870-W drive, showing complete suppression of the TE_{21} oscillation during the driver pulse.

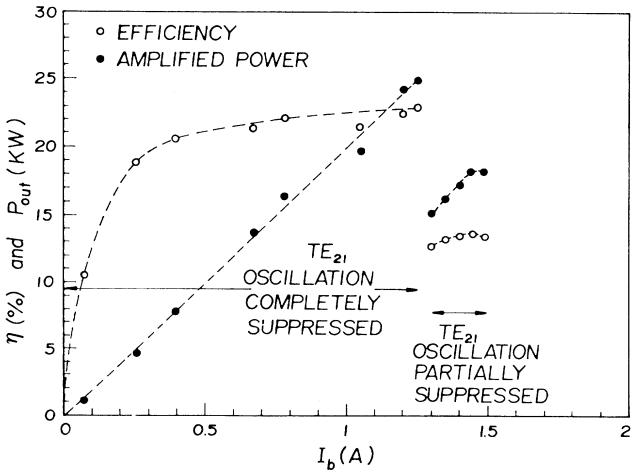

FIG. 4. P_{out} and η plotted as a function of beam current. $\eta \equiv P_{out}/P_{beam}$ for all data points except for $I_b = 0.076$ A where $\eta \equiv (P_{out} - P_{in})/P_{beam}$ to compensate for small gain. V_b, α, and B_0 are optimized for best η for $I_b \leq 1.25$ A, but stay constant for $I_b \geq 1.25$ A.

We interpret the observed mode competition and suppression qualitatively as follows. The *organized* beam perturbation associated with one mode would appear as a deleterious energy and velocity spread to another mode of different frequency or mode structure, and vice versa. Mode suppression occurs when one mode reaches such a level that its associated beam perturbation partially or completely stabilizes the competing mode, as in the case of high drive power. Driver-suppressed oscillation has also been reported in cyclotron-autoresonance-maser (CARM) simulations[13] (with no details given).

In summary, we have obtained good stability in a gyro-TWT in the operating (TE_{11}) mode. The dominant cause of oscillation was observed to be the absolute instability in the TE_{21} mode at the second cyclotron harmonic. Through specially designed couplers, the presence of mode competition and its effects on gain and efficiency were clearly demonstrated. Significantly, the TE_{21} oscillation was found to be suppressed by the application of the TE_{11} drive and complete suppression has been observed with beam currents up to at least 6 times the start-oscillation current. Greatly improved power and efficiency were obtained upon complete suppression of the absolute instability. The results provide an experimental verification of a new mechanism for the suppression of the absolute instability which has limited the power of gyro-TWT's and the expected power of several ongoing CARM amplifier projects aimed at ultrahigh power.

The authors gratefully acknowledge support from Professor N. C. Luhmann's group at University of California at Los Angeles, Electronic Research and Service Organization in Hsinchu, and the following individuals:

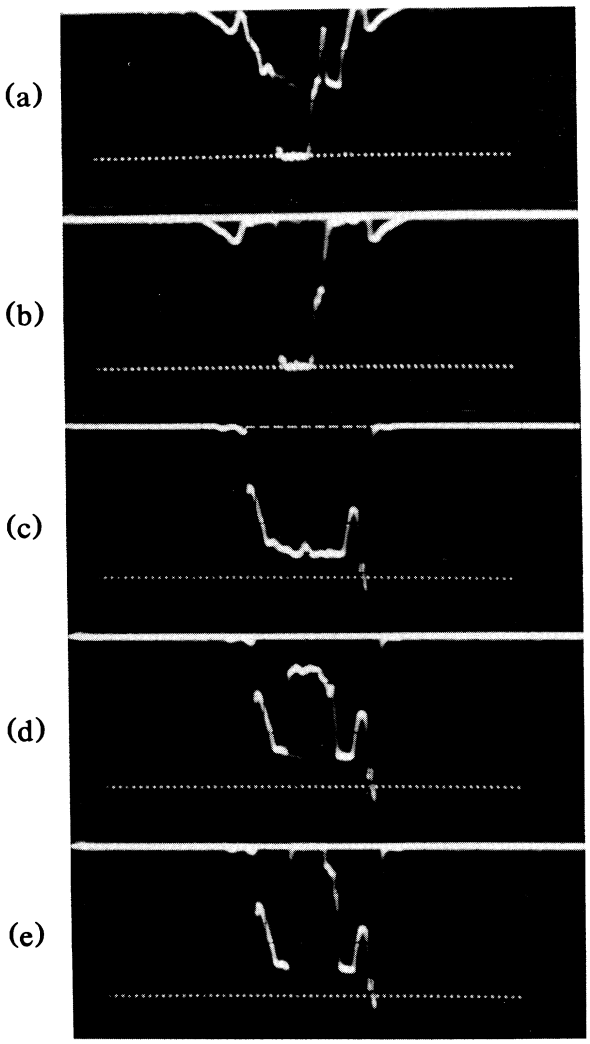

FIG. 5. Oscilloscope photos of the output signals. (a) and (b) are from port 1. (c)–(e) are from port 2. Each picture is the superposition of ~1000 pulses over 2.5 min.

Zuei Vin Hung, Yin Tung Chou, Hui Na Liu, Professor Juh Tzeng Lue, Tze Te Yang, Shu Shen Chang, Dr. Soo Yong Park, Kam Fai Chen, Dr. Jeff Arrington, and Chi Yao Chen. We also express our gratitude for a generous donation from Hewlett-Packard Taiwan Ltd. This work was sponsored by the National Science Council of the Republic of China.

[1]J. L. Seftor, V. L. Granatstein, K. R. Chu, P. Sprangle, and M. E. Read, IEEE J. Quantum Electron. **15**, 848 (1979).

[2]L. R. Barnett, K. R. Chu, J. M. Baird, V. L. Granatstein, and A. T. Drobot, in *Technical Digest of the International Electron Devices Meeting* (IEEE, New York, 1979), pp. 164–167.

[3]L. R. Barnett, J. M. Baird, Y. Y. Lau, K. R. Chu, and V. L. Granatstein, in *Technical Digest of the International Electron Devices Meeting* (IEEE, New York, 1980), pp. 314–317.

[4]R. S. Symons, H. R. Jory, S. J. Hegji, and P. E. Ferguson, IEEE Trans. Microwave Theory Tech. **29**, 181 (1981).

[5]P. E. Ferguson, G. Valier, and R. S. Symons, IEEE Trans. Microwave Theory Tech. **29**, 794 (1981).

[6]Howard Jory (private communication) [see also V. L. Granatstein and S. Y. Park, in *Technical Digest of the International Electron Devices Meeting* (IEEE, New York, 1983), pp. 263–266].

[7]Y. Y. Lau, K. R. Chu, L. R. Barnett, and V. L. Granatstein, Int. J. Infrared Millimeter Waves **2**, 373 (1981).

[8]K. R. Chu and A. T. Lin, IEEE Trans. Plasma Sci. **16**, 90 (1988).

[9]J. M. Baird and W. Lawson, Int. J. Electron. **61**, 953 (1986).

[10]Our MIG was designed by Hui Na Liu [Master thesis, National Tsing Hua University, 1988 (unpublished)].

[11]P. Sprangle and A. T. Drobot, IEEE Trans. Microwave Theory Tech. **25**, 528 (1977).

[12]K. R. Chu, A. T. Drobot, V. L. Granatstein, and J. L. Seftor, IEEE Trans. Microwave Theory Tech. **27**, 178 (1979).

[13]A. T. Lin and C. C. Lin, Int. J. Infrared Millimeter Waves **6**, 41 (1985).

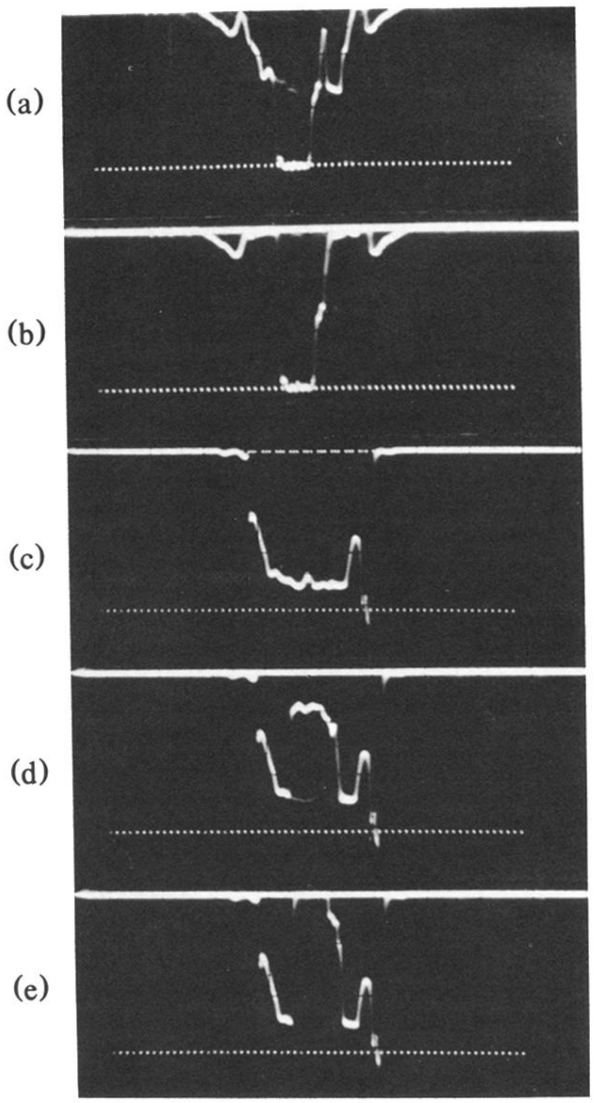

FIG. 5. Oscilloscope photos of the output signals. (a) and (b) are from port 1. (c)–(e) are from port 2. Each picture is the superposition of ~1000 pulses over 2.5 min.